Biodecolorization of Methylene Blue by Using *Bacillus subtilis* Immobilized into SA-PVA-Bentonite Matrix in Mineral Salt Medium and Non-nutritious Medium

Alya Awinatul Rohmah, Adi Setyo Purnomo*, and Widiya Nur Safitri

Department of Chemistry, Faculty of Science and Data Analytics, Institut Teknologi Sepuluh Nopember (ITS), Kampus ITS Sukolilo, Surabaya 60111, Indonesia

* ***Corresponding author:***

email: adi_setyo@chem.its.ac.id

Received: July 7, 2022
Accepted: September 23, 2022

DOI: 10.22146/ijc.76080

Abstract: *Industrial dye wastewater can potentially cause significant harm to organisms and the environment across the world. Methylene blue (MB) is a synthetic dye that can be found in wastewater. Immobilizing clay material and degradative bacteria into a carrier is the best way to remove MB. Therefore, this study aimed to immobilize* Bacillus subtilis *in sodium alginate (SA)-polyvinyl alcohol (PVA)-Bentonite for adsorption and degrading MB in nutritious mineral salt medium (MSM) and non-nutritious media. The result showed that SA-PVA-Bentonite-non-living* B. subtilis *beads (SPB-nBS) had the highest result in non-nutritious medium, approximately 88.89%. While in nutritious MSM, living* B. subtilis *addition into beads (SPB-BS) reached the highest MB removal, which was 94.31%. Nutritious MSM had a role as the sole carbon and energy for living* B. subtilis*. So, it could adsorb and degrade MB by its enzymatic system. The degradation products were predicted as $C_7H_{10}N_2O_4S$, $C_8H_{10}N_2O_2$ and $C_6H_8N_2O_3S$. Hence, this study indicated that a nutritious medium was the suitable medium for MB degradation. According to the SEM result, the bacteria spread and covered the beads. Furthermore, the adsorption kinetics and isotherms were also analyzed; SPB beads followed the pseudo-second order kinetic model and Langmuir isotherm.*

Keywords: *adsorption; immobilization;* Bacillus subtilis*; methylene blue*

■ INTRODUCTION

Currently, dye wastewater is a major environmental hazard since the effluents are mostly toxic and cannot degrade easily [1]. The world has produced 7×10^5 tons of dyes, and in the textile industry process, it is estimated that 10–15% was wasted through wastewater [2]. The accumulation of dye in the environment can disrupt the process of photosynthesis in waterbodies because it could retard light penetration from entering the waterbody. Additionally, dye wastewater can cause the environment to be less aesthetic [3]. Methylene blue (MB) is a synthetic and cationic dye for coloring specimens in laboratories and is used as a dye for silk, wool, and cotton fabrics [4]. Untreated MB wastewater could induce human health risks, such as cyanosis, eye irritation and digestive problems [5].

Handling MB dye wastewater treatment before being discharged directly into the environment is very important. Three methods can remove dye waste, including chemical, physical and biological methods [6]. The biological method uses the role of microbes (bacteria, fungi and microalgae), and it is environmentally friendly [7]. *Bacillus subtilis* is a species known to degrade synthetic dye wastewater and adsorb synthetic dyes [8-10]. *B. subtilis* can produce lignin peroxidase (LiP), NADH DCIP reductase and laccase enzymes that can degrade complex aromatic compounds into simpler compounds [11-12]. While living cells are more successful at biodegrading pollution, non-living cells are more effective in binding pollutants to the cell surface [13]. Non-living cells of bacteria, fungi, and microalgae have some advantages in adsorption pollutants in an aqueous medium. It does not require a lot of nutrients to survive, has a high pollution tolerance, and may have the quickest adsorption rate [14]. Unfortunately, it still has some drawbacks to using microbes through the free cell technique only, especially when it encounters environmental stress factors (pH,

temperature, and nutrient amount). Therefore, an appropriate strategy is required to preserve the microbe while still achieving efficient decolorization results, such as the immobilization technique with extra adsorbent materials [15].

The immobilization technique limits the movement of materials or microorganisms. It is used for pollutant remediation and has several advantages in cycle reusability, more resistance to the environment, and easy separating from the treatment solution [16]. It usually uses biodegradable sodium alginate (SA) which has high adsorption capacity [17]. Entrapment by cross-linked calcium alginate is the easiest way of immobilization [18] but has the drawback of less mechanical strength [15]. Additionally, polyvinyl alcohol (PVA) is a material also used for this process [19]. It can increase the mechanical strength of the matrix immobilization, but it could reduce mass transfer in the matrix system. The addition of Bentonite adsorbent filler material is the best solution to increase the mass transfer of the matrix and its adsorption capacity [15,20].

A previous study reported that Bentonite had been applied in alginate beads for MB removal [21]. At the same time, Ravi and Pandey [22] exhibited the adsorption capacity of alginate beads within Bentonite addition until 85% efficiency removal. On the other hand, the addition of *B. subtilis* showed that it could degrade the wastewater pollutant industry and become its secondary product [23]. Therefore, to enhance adsorption and degrading ability in the removal of MB wastewater, *B. subtilis* bacterium was immobilized into SA-PVA-Bentonite. The application was conducted in various aqueous mediums, which has nutrient source and limited nutrient composition. The bead's morphology was characterized by using SEM and FTIR for the functional group identification. Additionally, the adsorption kinetics and isotherms of the SA-PVA-Bentonite (SPB) beads were also studied.

■ EXPERIMENTAL SECTION

Materials

The strain of *B. subtilis* NBRC 3009 was obtained from the Microbial Chemistry Laboratory collection, Department of Chemistry, Institut Teknologi Sepuluh Nopember Surabaya, Indonesia. The growth media were Nutrient Agar (NA; Merck, Germany) and Luria Bertani Broth (LB; Merck, Germany). Methylene blue ($C_{16}H_{18}N_3SCl{\cdot}xH_2O$, MB) was purchased from Merck, Germany. Furthermore, this research also used sodium alginate (SA; Himedia, India), polyvinyl alcohol (PVA; Merck, Germany), Bentonite (PT. Bentonit Alam Indonesia), calcium chloride ($CaCl_2$; SAP Chemicals), demineralized water, and ethanol (70%) were purchased from UD. Sumber Ilmiah Persada Indonesia. Dipotassium phosphate (K_2HPO_4), monopotassium phosphate (KH_2PO_4), magnesium sulfate heptahydrate ($MgSO_4{\cdot}7H_2O$), sodium chloride (NaCl), iron(II) sulfate hexahydrate ($FeSO_4{\cdot}7H_2O$), ammonium nitrate (NH_4NO_3), calcium chloride dihydrate ($CaCl_2{\cdot}2H_2O$), and D-glucose ($C_6H_{12}O_6$) were purchased from Merck Germany and used for making MSM.

Instrumentation

This study used Vertical Steam Sterilizer LS-50LJ (GEA Medical; autoclave) for sterilizing, laminar airflow (Hotpack) and Incubator (LOVIBOND) for bacteria culture and incubation. The result treatment was analyzed by using UV-VIS Spectrophotometer Genesys 10s (Thermo Scientific) and Scanning Electron Microscopy (SEM) INSPECT-S50 (FEI). The degradation product was analyzed by using LC-TOF/MS (Bruker), with an ESI mass range of 50–1000 *m/z*. The column was Acclaim TM RSLC 120 C18, 2.1 × 100 mm, with a particle size of 2.2 µm at 33 °C.

Procedure

Bacteria culture preparation

B. subtilis was inoculated onto NA medium sterile in an agar plate by re-streaking, and the culture was incubated at 37 °C for 24 h inside an incubator. Furthermore, the culture of *B. subtilis* from NA was inoculated into a 20 mL LB broth liquid medium. The culture was pre-incubated for 24 h at 37 °C [24-25]. *B. subtilis* culture was streaked on sterile NA medium with MB 50 and 100 mg/L for biodecolorization MB on solid agar medium. The culture was then incubated at 37 °C for 1 and 3 days.

Matrix beads preparation and immobilization process

Matrix beads were synthesized from 0.5 g (1% w/v = g of solute/100 mL solution) SA, diluted in demineralized water by heating at 105 °C and stirred for an hour. Subsequently, SA hydrogel was added by 2 g (4% w/v) PVA and 0.5 g (1% w/v) Bentonite to make SPB hydrogel [15,26]. Furthermore, the hydrogel was stirred until it became homogeneous and was dropped into an 8 g (4% w/v) $CaCl_2$ solution using a sterile syringe. Afterward, formed beads were sunk into fresh $CaCl_2$ solution for crosslink until 24 h. The beads were washed with demineralized water three times to eliminate excess $CaCl_2$ [27].

Living and non-living cells of *B. subtilis* were immobilized in SPB gel before it was dropped into the $CaCl_2$ solution. Non-living *B. subtilis* was killed by the heating process at 121 °C for 15 min. The gel was homogenized by stirring for 30 min to ensure the bacteria's biomass was spread evenly [9,15]. The following technique was the same as the SPB beads procedure.

Methylene blue dye biodecolorization

SPB beads were applied to decolorize MB dye in a nutritious medium (Mineral Salt Medium/ MSM) and a non-nutritious medium (demineralized water). About 100 mL MB 50 mg/L in 250 mL Erlenmeyer flask which was diluted by MSM and non-MSM, were added by 32.5 mg beads, followed by incubation for 24 h at 30 °C under static conditions. After incubation, the supernatants were taken and analyzed using a spectrophotometer UV-Vis at 664 nm.

Furthermore, MB was also decolorized by using dried beads in a batch system for various initial weights of beads 10–30 mg within 5 mg intervals into 30 mg/L MB for 120 min under shaking conditions. In contrast, various time incubations were conducted by 20 mg beads into 30 mg/L MB for 5–240 min. Then various MB concentrations of 10, 20, 30, 40, 50, and 70 mg/L were decolorized by 20 mg beads for 180 min. All variation experiments were conducted in 20 mL non-nutritious medium under 30 °C and 120 rpm rotary shaker. The adsorption capacity of beads on MB decolorization was determined by using Eq. (1):

$$q_e = \frac{(c_0 - c_t)V}{W} \quad (1)$$

where c_0, q_e, and c_t are initial concentration, equilibrium concentration, and final concentration at a current time (mg/L), respectively, while V is the volume of MB solution (L), and W is the weight of beads (g).

Beads characterization

The functional group information of the synthesized immobilization beads was analyzed using FTIR at wave range 4000 until 400 cm^{-1}. SEM analyzed the surface and morphology of the beads before the MB adsorption treatment process. Before scanning by SEM, the beads were dried out by freeze-drying to remove all water contents. This analysis was also conducted for beads with and without bacteria addition (SPB-BS and SPB-nBS) [6].

Adsorption kinetics and isotherms study

Adsorption kinetic models were used to investigate the kinetics of beads adsorption. Furthermore, pseudo-first and pseudo-second order kinetic models are commonly used in adsorption kinetic models. This is shown by Eq. (2) and (3):

$$\ln(q_e - q_t) = \ln q_e - k_1 t \quad (2)$$

$$\frac{t}{q_t} = \frac{1}{k_2 q_e^2} + \left(\frac{1}{q_e}\right)t \quad (3)$$

where q_e and q_t are adsorption capacity at equilibrium and at a current time t (mg/g), k_1 is the pseudo-first order rate constant (min^{-1}), and k_2 is the pseudo-second order rate constant ($g.mg^{-1}.min^{-1}$).

The adsorption isotherms of MB into the beads were investigated using various MB initial concentrations. These were assessed by using the Langmuir and Freundlich models, which are represented by Eq. (4) and (5):

$$\frac{c_e}{q_e} = \frac{1}{K_L q_m} + \frac{c_e}{q_m} \quad (4)$$

$$\ln q_e = \ln K_f + \frac{1}{n}\ln c_e \quad (5)$$

where c_e is the equilibrium equation, q_m and q_e are maximum and equilibrium capacity (mg/g), K_L (mg/L) and K_f (mg/g) are Langmuir and Freundlich constants, respectively [28].

■ RESULTS AND DISCUSSION

Decolorization and Degradation of Methylene Blue in Solid Medium (Nutrient Agar)

B. subtilis was inoculated onto nutrient agar (NA) medium and observed for 1 and 3 days. The results were shown in Fig. 1(a) and 1(b), *B. subtilis* could grow on the first day at 50 and 100 mg/L MB. The faded blue color visual from decolorization zones proved that *B. subtilis* could survive in a medium with MB on the NA medium by secreting its enzymes [29]. NA consists of peptone, malt extract, and yeast extract that can be utilized as nutritional resources for bacteria, especially for its sole carbon and energy. Supported by its composition, such as amino acid, vitamin, and protein, nutrition could rapidly lead to the growth of bacteria, have the optimum capability to produce its colony, and enhance its potential enzymes secretion [30].

On the third day of incubation (Fig. 1(c) and 1(d)), the result showed that *B. subtilis* had been decolorized and degraded MB more clearly than on the first day (Fig. 1(a) and 1(b)). It was proved by the appearance in the middle of NA agar which is lighter than on the first day of incubation. In a previous study by Purnomo et al. [31], *B. subtilis* cell could decolorize 100 mg/L MB until 88.00% on the seventh day, followed by its decreasing MB color absorption in nutritious potato dextrose broth (PDB) medium.

Decolorization of Methylene Blue in Non-nutritious Liquid Medium and MSM

MB decolorization in a non-nutritious liquid medium was conducted using variation beads (SPB, SPB-nBS, and SPB-BS). The medium consisted of MB diluted with demineralized water. In a free environment, especially in wastewater treatment, the lack of nutrition and other stressing factors are commonly found, such as pH, temperature, and salinity. Those are essential concerns regarding the remediation of pollutants. It could affect the bead's ability to decolorize pollutants, especially adsorbent material supported by living microorganisms [9].

Various decolorization beads experiments were conducted by using 32.5 mg at 100 mL volume within

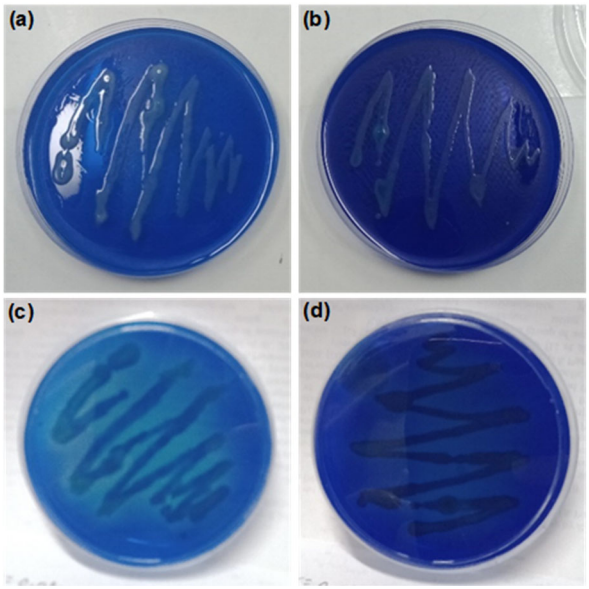

Fig 1. Decolorization and degradation of MB by *B. subtilis* on NA medium (a) 50 mg/L MB after 1 day, (b) 100 mg/L MB after 1 day, (c) 50 mg/L MB after 3 days, and (d) 100 mg/L MB after 3 days

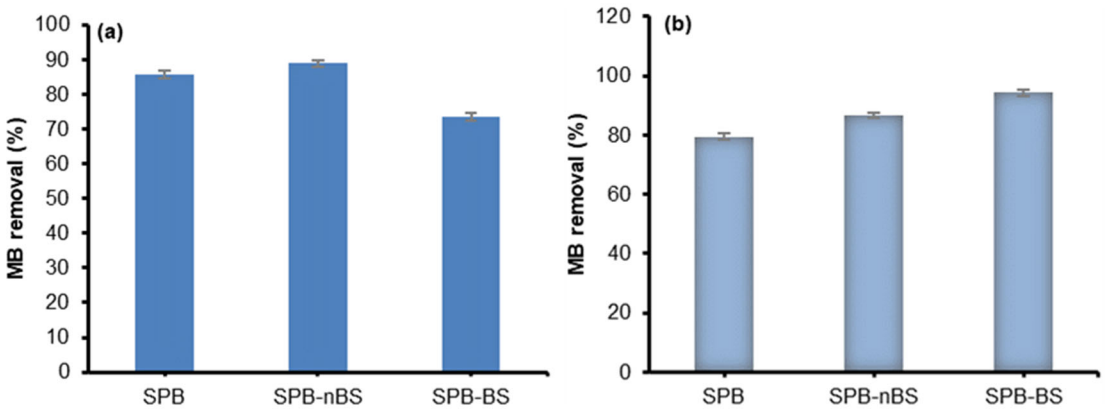

Fig 2. MB percent removal in (a) non-nutritious medium and (b) mineral salt medium (MSM)

50 mg/L MB concentration under 24 h. Fig. 2(a) showed MB removal in a non-nutritious liquid medium. SPB-BS beads could remove 73.56% MB, while SPB and SPB-nBS could decolorize MB to 85.67 and 88.89%, respectively. In addition, beads with SPB-nBS had a higher percent removal result than SPB-BS. The heating process made *B. subtilis* cells inactive [32]. Tural et al. [32] reported that the *B. subtilis* cell wall consists of peptidoglycan, which belongs to some of the functional groups (carboxylate anions ($-COO^-$), –NH, hydroxy (–OH), –C=O, –C–N–, –C–O, and –C–H). Hence, it could make interaction with some molecules such as MB. Meanwhile, it was reported that living cell bacteria also had a defense ability, especially *B. subtilis*, which could produce biofilm to protect its cell from the toxic environment, such as dye pollutants [33]. This biofilm inhibited MB in contact with *B. subtilis* cells due to the adaption of lacking nutrition and high toxicity medium.

At MB biodecolorization by beads in a medium which consists of nutrient/MSM, the MB removal (Fig. 2(b)) was different from the non-nutritious medium result (Fig. 2(a)). Fig. 2(b) showed that the highest MB removal was reached by SPB-BS at approximately 94.31%, followed by SPB-nBS and SPB, which decolorized MB to 86.60 and 79.40%, respectively. Nutrient amount composition has a crucial role in MB biodecolorization as a mineral and sole carbon source. Hence, *B. subtilis* bacteria needs some of those nutrients for growth, especially for enzyme secretion [34]. Those enzymes could degrade MB and become its degradation product. While, on SPB-nBS beads treatment, the bacteria did not produce the enzyme. The heating treatment process killed the bacteria and denatured its enzymes [31].

Adsorption and Degradation Mechanism

The mechanism in SPB and SPB-nBS beads experiments was adsorption, while the SPB-BS beads experiment was involved in adsorption and biodegradation. The matrix framework of the beads was formed by crosslinking between sodium alginate and calcium chloride ($CaCl_2$). Alginate is a biocompatible material commonly used in immobilization [35]. In addition, PVA and Bentonite were used as fillers which can bind through hydrogen bond interaction [36]. Fig. 3 showed that MB was adsorbed into the beads by hydrogen bond and electrostatic interaction. The electrostatic interaction was caused by the positive charge of MB and the negative charge of Bentonite. Bentonite has super-capacity in adsorbing MB because of its ionic exchange (cationic) and high adsorption capacity [15].

In this study, living *B. subtilis* has a role in degrading MB to become metabolite degradative products by its enzymatic system. Oxidoreductase enzymes are enzymes that could lead to the oxidation or

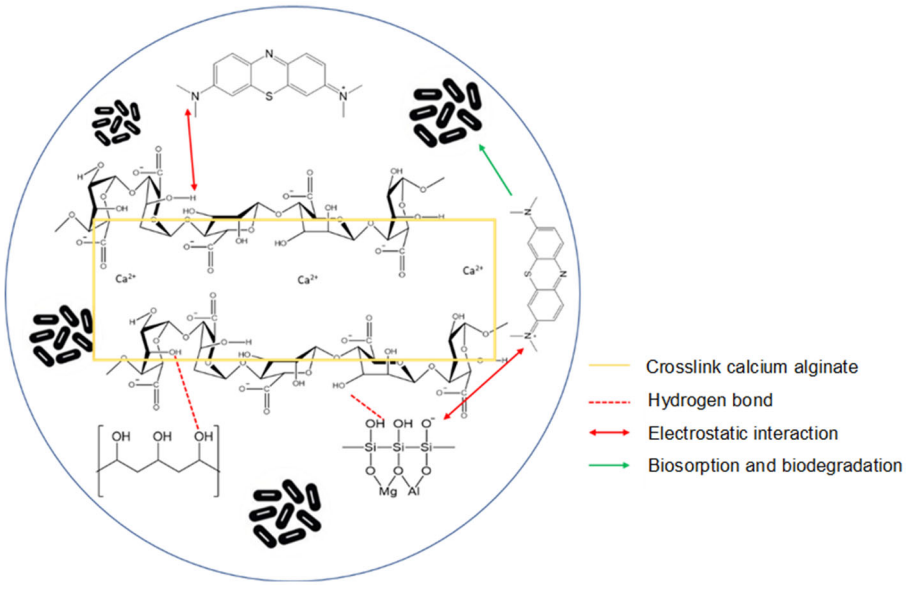

Fig 3. The interaction of MB with the beads

reduction process. *B. subtilis* is known to produce those enzymes. Laccase and lignin peroxidase (LiP) are a group of oxidation enzymes. A previous study reported that *B. subtilis* produced laccase identified by 2,2'-azino-bis(3-ethylthiazoline-6-sulfonate) (ABTS). This laccase decolorized 44.6 µg indigo carmine dye [37]. While another study reported, *B. subtilis* degraded reactive blue dye by LiP, azoreductase and NADH-DCIP reductase activity [11]. Azoreductase enzyme activity also could degrade mixed azo dyes (Reactive Red, Reactive Brown, and Reactive Black) [38]. In SPB-nBS beads, the degradation process was not found. Heat-killed bacteria (non-living *B. subtilis*) cannot degrade MB pollutants because high temperatures made its enzymes denatured [32].

MB degradation products were analyzed by using LC-MS. At 16.17 min retention time, the chromatogram control from SPB decolorization showed *m/z* 284, which was identified as MB (Fig. 4(a)). Then Fig. 4(b) showed the chromatogram of MB degradation by SPB-BS beads. The retention time of 4.32 and 8.93 min were shown as *m/z* 218 and 167, respectively. These degradation products were predicted as $C_7H_{10}N_2O_4S$ and $C_8H_{10}N_2O_2$ based on TiO_2/UV photocatalytic study by Houas et al. [39]. At the same time, a retention time of 11.17 min was predicted as $C_6H_8N_2O_3S$ (*m/z* 187), which was supported by Jia et al. [40] about MB degradation by novel ZnO/bone char composite. The chemical structure of metabolite product prediction was exhibited in Table 1.

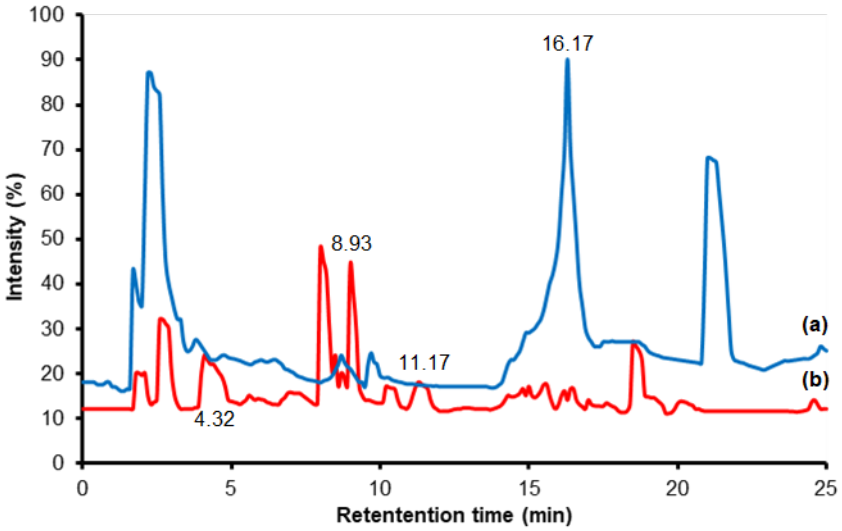

Fig 4. LC-MS result of MB degradation (a) SPB and (b) SPB-BS decolorization result

Table 1. Prediction of MB degradation metabolite products

Retention time (min)	*m/z*	Molecular formula	Structure
4.32	218	$C_7H_{10}N_2O_4S$	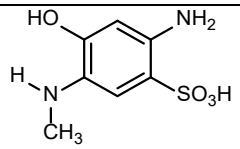
8.93	166	$C_8H_{10}N_2O_2$	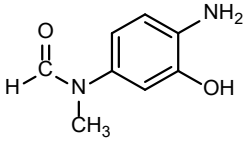
11.17	187	$C_6H_8N_2O_3S$	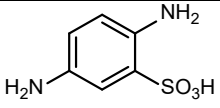

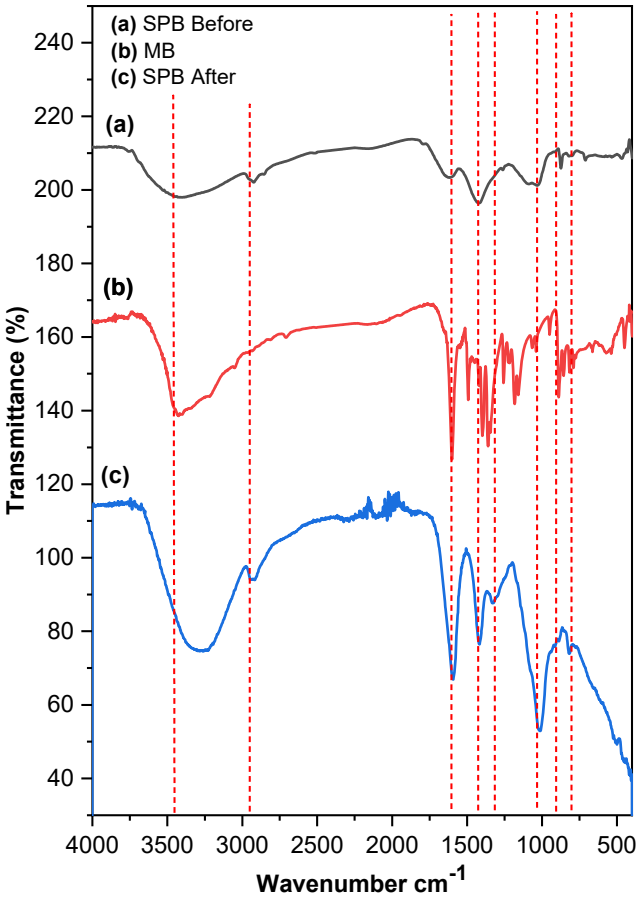

Fig 5. FTIR image of beads after and before adsorption

The mechanism of degradation by SPB-BS beads was through the chemisorption mechanism. The MB was degraded to become a simpler product by *B. subtilis* enzymatic mechanism.

Bead Analysis

Fourier transform infrared

Fig. 5(a) showed the FTIR results of SPB beads before MB decolorization, followed by control analysis (MB dye) and SPB beads after MB decolorization. SPB beads were composed of the combination SA; PVA; and Bentonite, proved by the presence of peak spectra at range O–H stretching (3700–3200 cm^{-1}); C–H stretching vibration (2900 cm^{-1}); stretching C=O and C–O (1700 nm^{-1}), and the combination functional groups (range 1400 and 1100 cm^{-1}). Si–O group stretching vibrations of Bentonite corresponded in the range of 950–1100 cm^{-1} and divided into a sharp band at 1033 cm^{-1} with a shoulder around 1088 cm^{-1} attributed to perpendicular Si–O stretching [36].

On MB FTIR result analysis, there are a significant peak at 2924 cm^{-1} refers to C–H asymmetric stretching, –NH stretching vibration at band 3443 cm^{-1}, C=C ring stretching figured at 1500 to 1400 cm^{-1}, CH=N at 1600 cm^{-1}, the $-CH_2$ or $-CH_3$ stretching at 1400 to 1300 cm^{-1}, and the –C–N and N–N stretching absorption peaks at 1252 and 1224 cm^{-1}, respectively (Fig. 5(b)) [41]. The C–H at 1176 cm^{-1}, C–N at 1146 cm^{-1}, C–S–C at 1064 cm^{-1}, and C–H out-of-plane bending vibrations of the ring at 881 and 824 cm^{-1} were the other MB absorption peaks [41].

After the MB adsorption process, the SPB beads FTIR result showed that there was spectra addition of MB (Fig. 5(c)). The combinations were shown at overlapping –OH and –NH spectra bands at 3200–3500 nm^{-1}. Based on LCMS analysis prediction, it showed that the functional group of metabolite products from SPB-BS beads was similar to the functional groups of MB and the beads themselves. Hence, FTIR spectra SPB beads after MB removal had the same peaks among MB and SPB beads.

Scanning electron microscopy

The morphology and topology structure of beads were characterized using Scanning Electron Microscopy (SEM). Fig. 6 showed SEM images of the bead's outer surface. SPB bead reported an irregular visual shape constructed by a mix of SA, PVA, and Bentonite (Fig. 6(a)) similar to SPB-BS and SPB-nBS beads (Fig. 6(c) and 6(e)). However, it showed that *B. subtilis* bacterium colony (rod shape) had been spread out on the bead's surface, which was different from the SPB beads (no bacteria). Heat-killed non-living bacteria were flatter than the living types (Fig. 6(c) and 6(e)). A previous study reported that *B. subtilis* had a maximum growth temperature of 53 °C [42]. After the MB adsorption process, beads were also analyzed by SEM, as shown in Fig. 6(b), 6(d), and 6(f), and the image showed the MB-covered bead's surface, represented by agglomeration. *B. subtilis* bacteria blocked MB transfusion in and out of the beads [15].

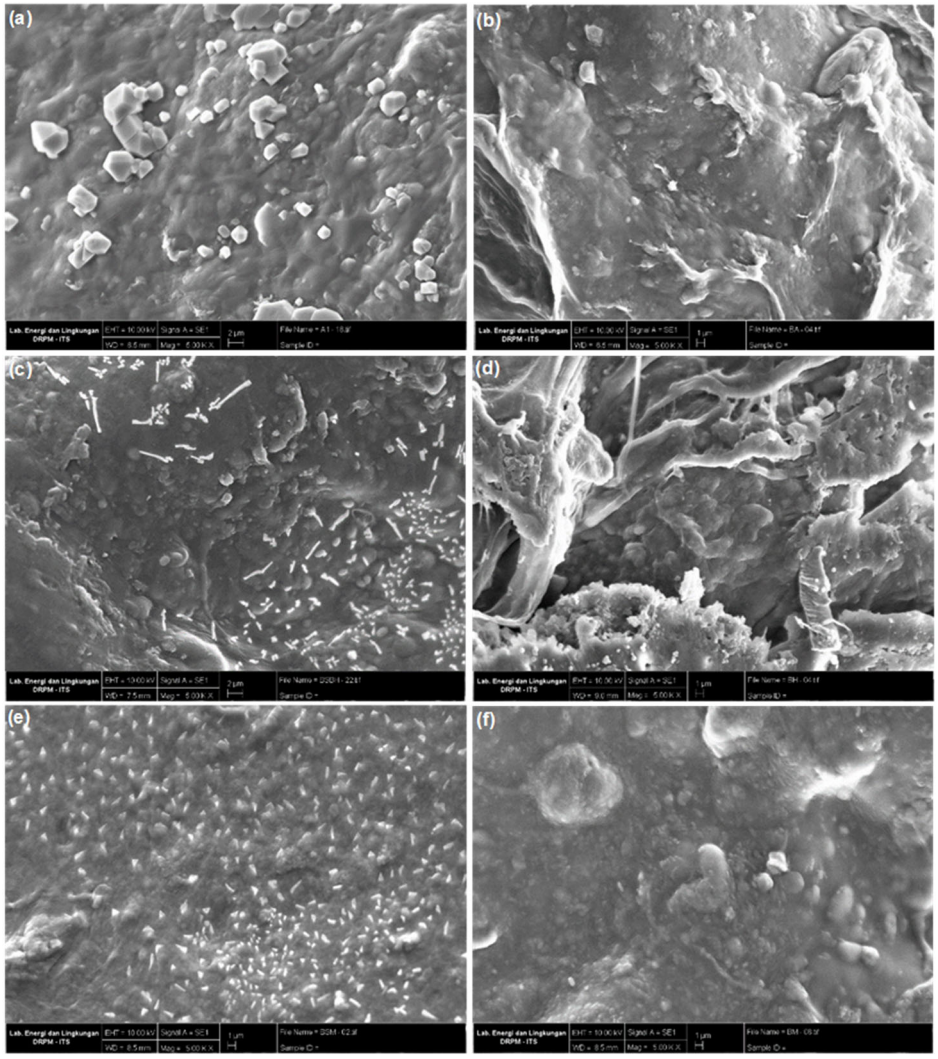

Fig 6. SEM images of the bead surface (a) SPB before, (b) SPB after, (c) SPB-BS before, (d) SPB BS after, (e) SPB-nBS before, and (f) SPB-nBS after MB adsorption

Adsorption Analysis of Dried Beads

Analysis of MB decolorization by various weights of dried beads mass was conducted on SPB, SPB-nBS, and SPB-BS beads (Fig. 7(a)). MB removal by SPB-BS beads was still increased, similar to SPB-nBS beads on 10–30 mg mass weight beads at 5 mg intervals. While SPB beads reached equilibrium at 20 mg mass weight in 30 mg/L MB solution at 120 min time shaking condition, estimated 62.10% within 19.25 mg/g adsorption capacity. The higher percent removal was obtained at 30 mg beads for SPB, SPB-BS, and SPB-nBS, estimated at 64.43, 53.98, and 60.26%, respectively. At 10 mg mass of weight beads, SPB-nBS beads had been adsorbed at 26.64%.

When various adsorption times were carried out, the equilibrium capacity was reached at 180 min, estimated at 23.78 mg/g adsorption capacity for SPB beads (Fig. 7(b)). The weight of beads in this analysis was 20 mg, and the MB concentration was 30 mg/L under 120 rpm shaking condition. Beads adsorption capacities were increased directly under 180 min. In addition, SPB-nBS and SPB-BS beads had higher capacity adsorption at 240 min incubation shaker time, 23.45 and 20.11 mg/g, respectively.

Various MB concentrations were conducted at 10, 20, 30, 40, 50, and 70 mg/L MB. At 30 mg/L, the adsorption capacity of SPB-BS, SPB-nBS, and SPB beads

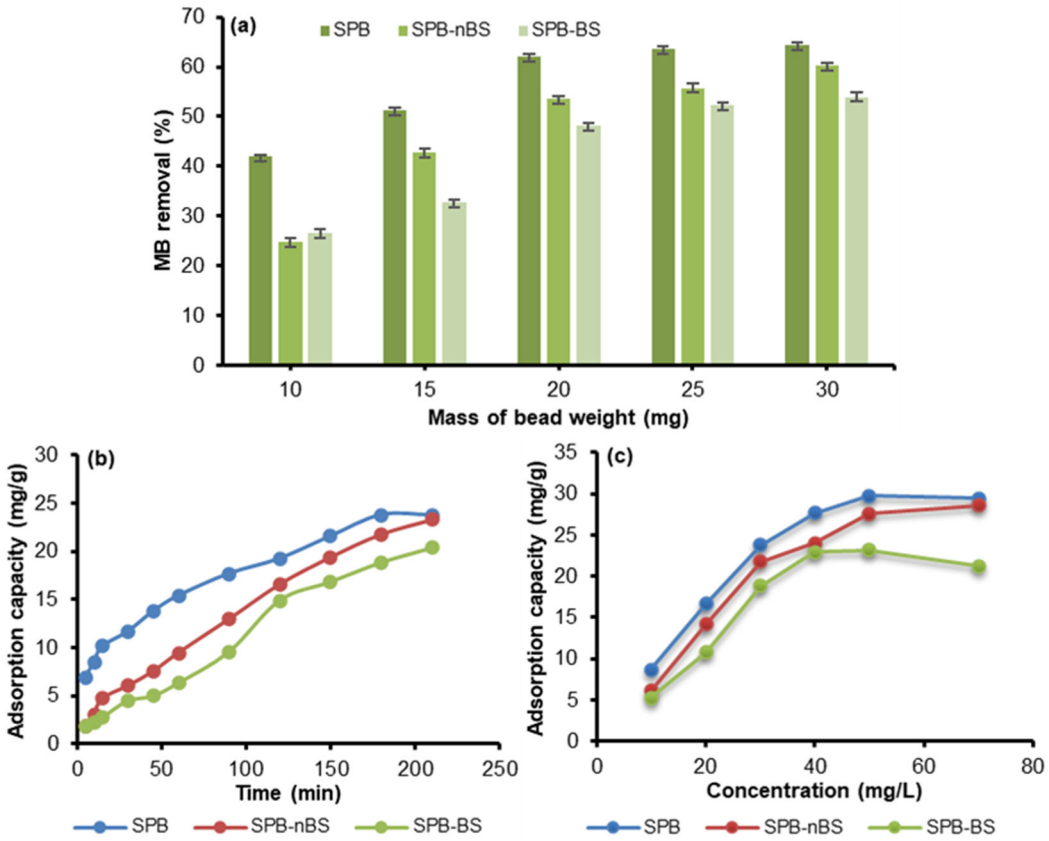

Fig 7. MB percent removal by (a) various beads weight, (b) various adsorption times, and (c) various MB concentrations

was 18.85, 21.76, and 23.78 mg/g, respectively. It was still increased to a 50 mg/L concentration of MB (Fig. 7(c)). Then at 70 mg/L, the SPB-BS beads after MB adsorption decreased to 21.25 mg/g. At MB concentrations of 40 and 50 mg/L, the adsorption capacities of SPB-BS beads were 22.95 and 23.16 mg/g, respectively.

Adsorption Kinetics

Adsorption kinetic reveals the equilibrium capacity and rate, which is influenced by the presence of active binding sites, the physicochemical nature of the adsorbent, and the specific surface area [43]. Chemical interaction between the adsorbate, mass transfer, bulk transfer, intraparticle diffusion, diffusion through micropores/macropores, and diffusion through the liquid film around the solid phase surface are all part of the mechanism [44]. The general adsorption process is dependent on the amount of adsorbate and the availability of adsorptive sites, according to pseudo-first and pseudo-second-order kinetic models [45].

Based on the linear graphics (Fig. 8(a) and 8(b)), the calculated values of K, q_e, and regression coefficient (R^2) were obtained and shown in Table 2. The regression coefficient of 0.981 with calculated q_e was 26.546 mg/g when the incubation was at a range of 5 until 240 min under the pseudo-first order kinetic. Therefore, this analysis can confirm that MB decolorization followed the pseudo-second order. Previous studies also reported that both pollutant adsorption by using PVA-SA-kaolin beads and calcium alginate-Bentonite/activated biochar followed pseudo-second order kinetics [46-47].

Adsorption Isotherms

The adsorption isotherm mechanism describes the distribution of adsorbate molecules in a solution between the solid and liquid phases at a particular system

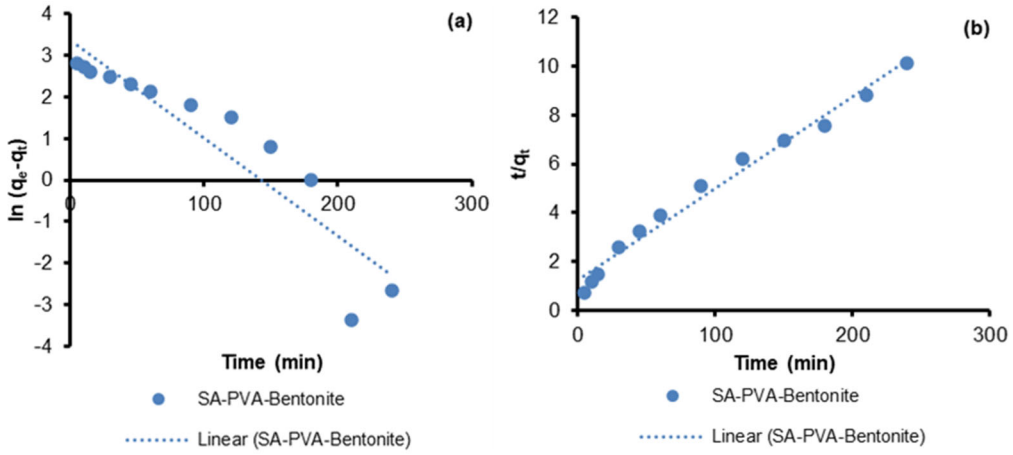

Fig 8. Graphic of (a) pseudo-first and (b) pseudo-second order kinetic models

Table 2. Kinetic parameters for adsorption of MB onto SPB beads based on different models

Pseudo-first order					Pseudo-second order				
R^2	Slope	Intercept	K_1	q_e cal	R^2	Slope	Intercept	K_2	q_e cal
0.861	-0.025	3.395	0.025	1.222	0.981	0.038	1.201	0.001	26.546

temperature. According to the Langmuir model, monolayer adsorption occurs on the adsorbent surface with similar homogeneous binding sites [48]. In contrast, the Freundlich model is based on the assumption of a heterogeneous distribution on the adsorbent surface [49]. The results showed that the regression coefficient (R^2) value of Langmuir isotherm was 0.973, with K_L of 0.238 and q_m of 37.010 mg/g (Fig. 9(a) and Table 3), while the regression coefficient (R^2) value of Freundlich isotherm was 0.803 (Fig. 9(b) and Table 3). These indicated that the varied Langmuir isotherm is applicable in this study. Therefore, MB adsorption by SA-PVA-Bentonite bead materials was conducted by monolayer adsorption.

Comparison with Other Biosorbents

Table 4 compared the biosorption capabilities of various biosorbents for the elimination of MB. In comparison to those described in the literature, dried SPB

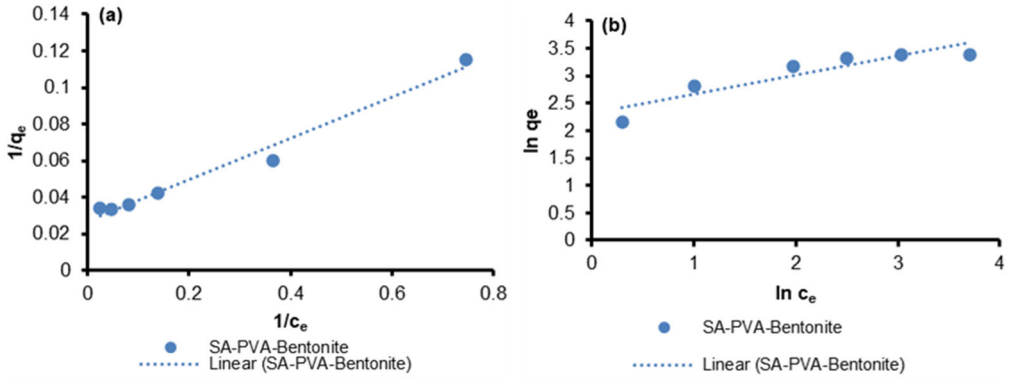

Fig 9. Graphic of (a) Langmuir and (b) Freundlich adsorption isotherms

Table 3. Isotherm adsorption analysis of MB onto SPB beads, according to Langmuir and Freundlich models

Langmuir isotherm					Freundlich isotherm				
R^2	Slope	Intercept	K_L	q_m	R^2	Slope	Intercept	K_F	n
0.973	0.113	0.027	0.238	37.010	0.803	0.349	2.312	205.112	2.866

Table 4. Comparison of biosorption capacities of various biosorbents for MB removal

Adsorbent	Adsorption capacity (mg/g)	References
Alginate-polyvinyl alcohol-Bentonite beads	37.01	Present study
Ca-alginate-Bentonite/biochar	47.39	[47]
PVA–Alginate/Bentonite nanocomposite hydrogel	51.37	[36]
polyvinyl alcohol/Bentonite hydrogels	27.90	[50]
Fe-sludge biochar	29.13	[51]
Alginate-graphene oxide beads	8.36	[52]
Magnetic/Activated Charcoal/β-Cyclodextrin/Alginate Polymer Nanocomposite	2.08	[53]

beads have a significant biosorption capacity.

■ CONCLUSION

In this study, *B. subtilis* was immobilized in the SA-PVA-Bentonite matrix to decolorize MB. The experiments were conducted under a non-nutritious medium and MSM. SPB-BS beads had the highest removal result in MB solution within MSM, approximately 94.31% for 24 h at 30 °C under static conditions. MSM was utilized by bacteria as the sole carbon and energy. The degradation products were predicted as $C_7H_{10}N_2O_4S$, $C_8H_{10}N_2O_2$ and $C_6H_8N_2O_3S$. While in the non-nutritious medium, non-living *B. subtilis* addition beads (SPB-nBS) reached the highest MB removal, which was 88.89%. SEM characterization showed that *B. subtilis* covered the surface of the beads. In addition, SPB beads were followed by pseudo-second order (K_2 0.001 and q_e 26.546 mg/g), and Langmuir isotherm (K_L 0.238 and q_m 37.010 mg/g).

■ ACKNOWLEDGMENTS

This study was supported by the Directorate of Research, Technology, and Community Service, Ministry of Education, Culture, Research and Technology of Indonesia in accordance with the Student Thesis Research Scheme 2022, Number: 084/E5/PG.02.00.PT/2022 with Researcher Contract Number: 1433/PKS/ITS/2022.

■ REFERENCES

[1] Gao, T., Guan, G., Wang, X., and Lou, T., 2022, Electrospun molecularly imprinted sodium alginate/polyethylene oxide nanofibrous membranes for selective adsorption of methylene blue, *Int. J. Biol. Macromol.*, 207, 62–71.

[2] Boumediene, M., Benaïssa, H., George, B., Molina, S., and Merlin, A., 2018, Effects of pH and ionic strength on methylene blue removal from synthetic aqueous solutions by sorption onto orange peel and desorption study, *J. Mater. Environ. Sci.*, 9 (6), 1700–1711.

[3] Rajabi, M., Mahanpoor, K., and Moradi, O., 2017, Removal of dye molecules from aqueous solution by carbon nanotubes and carbon nanotube functional groups: Critical review, *RSC Adv.*, 7 (74), 47083–47090.

[4] Zhi, S., Tian, L., Li, N., and Zhang, K., 2018, A novel system of MnO_2-mullite-cordierite composite particle with NaClO for Methylene blue decolorization, *J. Environ. Manage.*, 213, 392–399.

[5] Naushad, M., Alqadami, A.A., AlOthman, Z.A., Alsohaimi, I.H., Algamdi, M.S., and Aldawsari, A.M., 2019, Adsorption kinetics, isotherm and reusability studies for the removal of cationic dye from aqueous medium using arginine modified activated carbon, *J. Mol. Liq.*, 293, 111442.

[6] Rizqi, H.D., and Purnomo, A.S., 2017, The ability of brown-rot fungus *Daedalea dickinsii* to decolorize and transform methylene blue dye, *World J. Microbiol. Biotechnol.*, 33 (5), 92.

[7] Purnomo, A.S., Asranudin, A., Prasetyoko, D., and Azizah, Y.D.N., 2021, The biotransformation and biodecolorization of methylene blue by xenobiotic bacterium *Ralstonia pickettii*, *Indones. J. Chem.*, 21 (6), 1418–1430.

[8] Purnomo, A.S., Rizqi, H.D., and Harmelia, L., 2020, Culture of bacterium *Bacillus subtilis* as degradation agent in attempt of sea water remediation contaminated by petroleum, *J. Indones. Chem. Soc.*, 3 (1), 53–58.

[9] Upendar, G., Dutta, S., Chakraborty, J., and Bhattacharyya, P., 2016, Removal of methylene blue

dye using immobilized *Bacillus subtilis* in batch & column reactor, *Mater. Today: Proc.*, 3 (10), 3467–3472.

[10] Boelan, E.G., and Purnomo, A.S., 2018, Abilities of co-cultures of white-rot fungus *Ganoderma lingzhi* and bacteria *Bacillus subtilis* on biodegradation DDT, *J. Phys.: Conf. Ser.*, 1095, 012015.

[11] Barathi, S., Aruljothi, K.N., Karthik, C., and Padikasan, I.A., 2020, Optimization for enhanced ecofriendly decolorization and detoxification of Reactive Blue160 textile dye by *Bacillus subtilis*, *Biotechnol. Rep.*, 28, e00522.

[12] Mahmood, F., Shahid, M., Hussain, S., Shahzad, T., Tahir, M., Ijaz, M., Hussain, A., Mahmood, K., Imran, M., and Babar, S.A.K., 2017, Potential plant growth-promoting strain *Bacillus* sp. SR-2-1/1 decolorized azo dyes through NADH-ubiquinone:oxidoreductase activity, *Bioresour. Technol.*, 235, 176–184.

[13] Zuorro, A., Maffei, G., and Lavecchia, R., 2017, Kinetic modeling of azo dye adsorption on non-living cells of *Nannochloropsis oceanica*, *J. Environ. Chem. Eng.*, 5 (4), 4121–4127.

[14] Michalak, I., Chojnacka, K., and Witek-Krowiak, A., 2013, State of the art for the biosorption process - A review, *Appl. Biochem. Biotechnol.*, 170 (6), 1389–1416.

[15] Zhang, Y., Yu, Z., Hu, Y., Song, C., Li, F., He, W., Wang, X., Li, Z., and Lin, H., 2021, Immobilization of nitrifying bacteria in magnetic PVA–SA-diatomite carrier for efficient removal of NH_4^+-N from effluents, *Environ. Technol. Innovation*, 22, 101407.

[16] Ruan, B., Wu, P., Chen, M., Lai, X., Chen, L., Yu, L., Gong, B., Kang, C., Dang, Z., Shi, Z., and Liu, Z., 2018, Immobilization of *Sphingomonas* sp. GY2B in polyvinyl alcohol–alginate–kaolin beads for efficient degradation of phenol against unfavorable environmental factors, *Ecotoxicol. Environ. Saf.*, 162, 103–111.

[17] Xue, J., Wu, Y., Shi, K., Xiao, X., Gao, Y., Li, L., and Qiao, Y., 2019, Study on the degradation performance and kinetics of immobilized cells in straw-alginate beads in marine environment, *Bioresour. Technol.*, 280, 88–94.

[18] Purnaningtyas, M.A.K., Sudiono, S., and Siswanta, D., 2020, Synthesis of activated carbon/chitosan/alginate beads powder as an adsorbent for methylene blue and methyl violet 2B dyes, *Indones. J. Chem.*, 20 (5), 1119–1130.

[19] Rezvani, M.A., Oveisi, M., and Nia Asli, M.A., 2015, Phosphotungestovanadate immobilized on PVA as an efficient and reusable nano catalyst for oxidative desulphurization of gasoline, *J. Mol. Catal. A: Chem.*, 410, 121–132.

[20] Vezentsev, A.I., Thuy, D.M., Goldovskaya-Peristaya, L.F., and Glukhareva, N.A., 2018, Adsorption of methylene blue on the composite sorbent based on bentonite-like clay and hydroxyapatite, *Indones. J. Chem.*, 18 (4), 733–741.

[21] Belhouchat, N., Zaghouane-Boudiaf, H., and Viseras, C., 2017, Removal of anionic and cationic dyes from aqueous solution with activated organo-bentonite/sodium alginate encapsulated beads, *Appl. Clay Sci.*, 135, 9–15.

[22] Ravi, R., and Pandey, L.M., 2019, Enhanced adsorption capacity of designed bentonite and alginate beads for the effective removal of methylene blue, *Appl. Clay Sci.*, 169, 102–111.

[23] Su, C., Sun, X., Mu, Y., Li, P., Li, J., Fan, P., Zhang, M., Wang, M., Chen, X., and Feng, C., 2021, Multilayer calcium alginate beads containing diatom biosilica and *Bacillus subtilis* as microecologics for sewage treatment, *Carbohydr. Polym.*, 256, 117603.

[24] Purnomo, A.S., Andyani, N.E.A., Nawfa, R., and Putra, S.R., 2020, Fenton reaction involvement on methyl orange biodegradation by brown-rot fungus *Gloeophyllum trabeum*, *AIP Conf. Proc.*, 2237, 020002.

[25] Purnomo, A.A., Rizqi, H.D., Fatmawati, S., Putro, H.S., and Kamei, I., 2018, Effects of bacterium *Ralstonia pickettii* addition on DDT biodegradation by *Daedalea dickinsii*, *Res. J. Chem. Environ.*, 22, 151–156.

[26] Chen, W., Zhang, H., Zhang, M., Shen, X., Zhang, X., Wu, F., Hu, J., Wang, B., and Wang, X., 2021, Removal of PAHs at high concentrations in a soil washing solution containing TX-100 via simultaneous sorption and biodegradation processes by immobilized degrading bacteria in PVA-SA hydrogel beads, *J. Hazard. Mater.*, 410, 124533.

[27] Yuliana, M., Ismadji, S., Lie, J., Santoso, S.P., Soetaredjo, F.E., Waworuntu, G., Putro, J.N., and Wijaya, C.J., 2021, Low-cost structured alginate-immobilized bentonite beads designed for an effective removal of persistent antibiotics from aqueous solution, *Environ. Res.*, 207, 112162.

[28] Hasan, R., Ying, W.J., Cheng, C.C., Jaafar, N.F., Jusoh, R., Abdul Jalil, A., and Setiabudi, H.D., 2020, Methylene blue adsorption onto cockle shells-treated banana pith: Optimization, isotherm, kinetic, and thermodynamic studies, *Indones. J. Chem.*, 20 (2), 368–378.

[29] Kishor, R., Purchase, D., Saratale, G.D., Saratale, R.G., Ferreira, L.F.R., Bilal, M., Chandra, R., and Bharagava, R.N., 2021, Ecotoxicological and health concerns of persistent coloring pollutants of textile industry wastewater and treatment approaches for environmental safety, *J. Environ. Chem. Eng.*, 9 (2), 105012.

[30] Obase, K., 2019, Extending the hyphal area of the ectomycorrhizal fungus *Laccaria parva* co-cultured with ectomycorrhizosphere bacteria on nutrient agar plate, *Mycoscience*, 60 (2), 95–101.

[31] Purnomo, A.S., Rohmah, A.A., Rizqi, H.D., Putro, H.S., and Nawfa, R., 2021, Biodecolorization of methylene blue by mixed cultures of brown-rot fungus *Gloeophyllum trabeum* and bacterium *Bacillus subtilis*, *AIP Conf. Proc.*, 2370, 040006.

[32] Tural, B., Ertaş, E., Enez, B., Fincan, S.A., and Tural, S., 2017, Preparation and characterization of a novel magnetic biosorbent functionalized with biomass of *Bacillus subtilis*: Kinetic and isotherm studies of biosorption processes in the removal of methylene blue, *J. Environ. Chem. Eng.*, 5 (5), 4795–4802.

[33] Mohsin, M.Z., Omer, R., Huang, J., Mohsin, A., Guo, M., Qian, J., and Zhuang, Y., 2021, Advances in engineered *Bacillus subtilis* biofilms and spores, and their applications in bioremediation, biocatalysis, and biomaterials, *Synth. Syst. Biotechnol.*, 6 (3), 180–191.

[34] Kishor, R., Saratale, G.D., Saratale, R.G., Romanholo Ferreira, L.F., Bilal, M., Iqbal, H.M.N., and Bharagava, R.N., 2021, Efficient degradation and detoxification of methylene blue dye by a newly isolated ligninolytic enzyme producing bacterium *Bacillus albus* MW407057, *Colloids Surf., B*, 206, 111947.

[35] Maniyam, M.N., Hari, M., and Yaacob, N.S., 2020, Enhanced methylene blue decolourization by *Rhodococcus* strain UCC 0003 grown in banana peel agricultural waste through response surface methodology, *Biocatal. Agric. Biotechnol.*, 23, 101486.

[36] Aljar, M.A.A., Rashdan, S., and El-Fattah, A.A., 2021, Environmentally friendly polyvinyl alcohol–alginate/bentonite semi-interpenetrating polymer network nanocomposite hydrogel beads as an efficient adsorbent for the removal of methylene blue from aqueous solution, *Polymers*, 13 (22), 4000.

[37] Cho, E.A., Seo, J., Lee, D.W., and Pan, J.G., 2011, Decolorization of indigo carmine by laccase displayed on *Bacillus subtilis* spores, *Enzyme Microb. Technol.*, 49 (1), 100–104.

[38] Krithika, A., Gayathri, K.V., Kumar, D.T., and Doss, C.G.P., 2021, Mixed azo dyes degradation by an intracellular azoreductase enzyme from alkaliphilic *Bacillus subtilis*: A molecular docking study, *Arch. Microbiol.*, 203 (6), 3033–3044.

[39] Houas, A., Lachheb, H., Ksibi, M., Elaloui, E., Guillard, C., and Herrmann, J.M., 2001, Photocatalytic degradation pathway of methylene blue in water, *Appl. Catal., B*, 31 (2), 145–157.

[40] Jia, P., Tan, H., Liu, K., and Gao, W., 2018, Synthesis, characterization and photocatalytic property of novel ZnO/bone char composite, *Mater. Res. Bull.*, 102, 45–50.

[41] Alshehri, A.A., and Malik, M.A., 2019, Biogenic fabrication of ZnO nanoparticles using *Trigonella*

foenum-graecum (Fenugreek) for proficient photocatalytic degradation of methylene blue under UV irradiation, *J. Mater. Sci.: Mater. Electron.*, 30 (17), 16156–16173.

[42] Hong, E., Jeong, M.S., Kim, T.H., Lee, J.H., Cho, J.H., and Lee, K.S., 2019, Development of coupled biokinetic and thermal model to optimize cold-water microbial enhanced oil recovery (MEOR) in homogenous reservoir, *Sustainability*, 11 (6), 1652.

[43] Bhattacharyya, K.G., and Sharma, A., 2004, *Azadirachta indica* leaf powder as an effective biosorbent for dyes: A case study with aqueous Congo red solutions, *J. Environ. Manage.*, 71 (3), 217–229.

[44] Kooh, M.R.R., Dahri, M.K., Lim, L.B.L., Lim, L.H., and Malik, O.A., 2016, Batch adsorption studies of the removal of methyl violet 2B by soya bean waste: Isotherm, kinetics and artificial neural network modelling, *Environ. Earth Sci.*, 75 (9), 783.

[45] Aljeboree, A.M., Alshirifi, A.N., and Alkaim, A.F., 2017, Kinetics and equilibrium study for the adsorption of textile dyes on coconut shell activated carbon, *Arabian J. Chem.*, 10, S3381–S3393.

[46] Sun, Y., Cheng, S., Lin, Z., Yang, J., Li, C., and Gu, R., 2020, Combination of plasma oxidation process with microbial fuel cell for mineralizing methylene blue with high energy efficiency, *J. Hazard. Mater.*, 384, 121307.

[47] Das, L., Saha, N., Ganguli, A., Das, P., Bhowal, A., and Bhattacharjee, C., 2021, Calcium alginate–bentonite/activated biochar composite beads for removal of dye and biodegradation of dye-loaded composite after use: Synthesis, removal, mathematical modeling and biodegradation kinetics, *Environ. Technol. Innovation*, 24, 101955.

[48] Langmuir, I., 1918, The adsorption of gases on plane surfaces of glass, mica and platinum, *J. Am. Chem. Soc.*, 40 (9), 1361–1403.

[49] Freundlich, H., and Heller, W., 1939, The adsorption of *cis*- and *trans*-azobenzene, *J. Am. Chem. Soc.*, 61 (8), 2228–2230.

[50] Sanchez, L.M., Ollier, R.P., and Alvarez, V.A., 2019, Sorption behavior of polyvinyl alcohol/bentonite hydrogels for dyes removal, *J. Polym. Res.*, 26 (6), 142.

[51] Ahmad, A., Singh, A.P., Khan, N., Chowdhary, P., Giri, B.S., Varjani, S., and Chaturvedi, P., 2021, Bio-composite of Fe-sludge biochar immobilized with *Bacillus* sp. in packed column for bio-adsorption of methylene blue in a hybrid treatment system: Isotherm and kinetic evaluation, *Environ. Technol. Innovation*, 23, 101734.

[52] Wan Ibrahim, W.N., Zainal Abidin, N.H., Mohamad Hanapi, N.S., Ab Malek, N.F., Wan Sudin, W.N.A., Saim, N., and Rusmin, R., 2019, Adsorption studies of methylene blue by encapsulated nano-carbonaceous alginate beads, *Int. J. Eng. Technol.*, 7 (4.14), 210–215.

[53] Yadav, S., Asthana, A., Chakraborty, R., Jain, B., Singh, A.K., Carabineiro, S.A.C., and Susan, M.A.B.H., 2020, Cationic dye removal using novel magnetic/activated charcoal/β-cyclodextrin/alginate polymer nanocomposite, *Nanomaterials*, 10 (1), 170.